Synthesis, characterisation and redox behaviour of isocyanide incorporated, chalcogen stabilised mixed-metal clusters ☆

Pradeep Mathur [a,*], Saurav Chatterjee [a], Goutam K. Lahiri [a], Soma Chakraborty [a], John H. Kaldis [b], Michael J. McGlinchey [c,*]

[a] *Department of Chemistry, Indian Institute of Technology, Powai, Bombay 400 076, India*
[b] *Department of Chemistry, McMaster University, Hamilton, Ont., Canada L8S 4M1*
[c] *Department of Chemistry, University College Dublin, Belfield, Dublin 4, Ireland*

Abstract

Room temperature reaction of a benzene solution of $[Cp_2Mo_2Fe_2(CO)_7(\mu_3\text{-}E)(\mu_3\text{-}E')]$ ($EE' = Se_2$ (**1**), STe (**2**), SeTe (**3**)) with Pr^iNC or Bu^tNC resulted in the formation of iron bonded isocyanide clusters $[Cp_2Mo_2Fe_2(RNC)(CO)_6(\mu_3\text{-}E)(\mu_3\text{-}E')]$, [E = E′ = Se, R = Pr^i (**5**) or Bu^t (**9**); E = S, E′ = Te, R = Pr^i (**6a, 6b**) or R = Bu^t (**10a, 10b**); E = Se, E′ = Te, R = Pr^i (**7a, 7b**) or R = Bu^t (**11a, 11b**)] and molybdenum bonded isocyanide clusters $[Cp_2(RNC)Mo_2Fe_2(CO)_6(\mu_3\text{-}E)(\mu_3\text{-}E')]$, [E = E′ = Se, R = Pr^i(**13**) or Bu^t (**17**); E = S, E′ = Te, R = Pr^i (**14**) or R = Bu^t, (**18**); E = Se, E′ = Te, R = Pr^i (**15**) or R = Bu^t (**19**)]. Two isomers (**a** and **b**) were detected by ^1H NMR spectroscopy for the mixed-chalcogen clusters **6**, **7**, **10** and **11**, where the isocyanide group is bonded to an iron atom. Thermolytic reaction conditions were necessary for the reaction of $[(\eta^5\text{-}C_5H_5)_2Mo_2Fe_2(CO)_7(\mu_3\text{-}Te)_2]$ (**4**) with Pr^i NC or Bu^t NC to give $[Cp_2Mo_2Fe_2(RNC)(CO)_6(\mu_3\text{-}Te)_2]$ (R = Pr^i (**8**) or R = Bu^t, (**12**)) and $[Cp_2(RNC)Mo_2Fe_2(CO)_6(\mu_3\text{-}Te)_2]$ (R = Pr^i (**8**)). Compounds **5**–**19** have been characterised by IR and ^1H and ^{13}C NMR spectroscopy. The Se- and Te-bridged compounds have been further characterised by ^{77}Se and ^{125}Te NMR spectroscopy. The structures of compounds **12** and **14** were determined by single crystal X-ray diffraction methods. Redox properties of the mixed-metal clusters, **2**, **6**, **8**, **12** and **14** have been studied by cyclic voltammetry in the potential range ±2.5 V at 298 K, using a platinum working electrode.

Keywords: Cluster; Mixed metal; Carbonyl; Isonitrile; X-ray diffraction

1. Introduction

As part of our ongoing interest in developing facile synthetic methods for the preparation of mixed-metal clusters, we isolated clusters of the type $[Cp_2Mo_2Fe_2(CO)_7(\mu_3\text{-}E)(\mu_3\text{-}E')]$, (where E and E′ are chalcogen atoms) from the reaction of $[Fe_3(CO)_9(\mu_3\text{-}E)(\mu_3\text{-}E')]$ with $[Cp_2Mo_2(CO)_6]$ [1–4]. Some reactivity studies of this cluster type have already been described. For instance, $[Cp_2Mo_2Fe_2(CO)_7(\mu_3\text{-}E)(\mu_3\text{-}E')]$ reacts with chalcogen powder (E″) to form the clusters, $[Cp_2Mo_2Fe_2(CO)_6(E)(E')(E'')]$, in which two chalcogen atoms are triply bridging and the third quadruply bridging [3]. Under aerobic conditions, $[Cp_2Mo_2Fe_2(CO)_7(\mu_3\text{-}Te)_2]$ reacts with phenylazide to form the imido-bridged dimolybdenum compound, $[Cp_2Mo_2(O)_2(\mu\text{-}Te)(\mu\text{-}NPh)]$ [5]. Reflux of a benzene solution of $[Cp_2Mo_2Fe_2(CO)_7(\mu_3\text{-}S)(\mu_3\text{-}Te)]$, in the presence of air, forms the oxo-species, *trans*-$[Cp_2Mo_2(O)_2(\mu\text{-}O)(\mu\text{-}Te)]$ and *cis*-$[Cp_2Mo_2(O)_2(\mu\text{-}O)(\mu\text{-}S)]$ [6], while under anaerobic conditions, in presence of PhSH, the hydride-bridged cluster$[Cp_2Mo_2Fe_2(CO)_5(\mu_3\text{-}S)(\mu_3\text{-}Te)(\mu\text{-}SPh)(\mu_3\text{-}H)]$ is formed, which converts to the dimolybdenum compound $[Cp_2Mo_2(\mu\text{-}S)(\mu\text{-}Te)(\mu\text{-}SPh)_2]$ on extended thermolysis [7]. Ligand substitution reactions form an interesting aspect of the overall study of reactivity in mixed-metal clusters. In this regard, we chose to look at

the reactions of $[Cp_2Mo_2Fe_2(CO)_7(\mu_3\text{-}E)(\mu_3\text{-}E')]$ with the isocyanide functionality as the cluster contains a variety of interesting structural features: three types of carbonyl groups, a heterometallic system containing two different metal atoms, and a pair of bridging chalcogen atoms which can be varied amongst S, Se and Te. While our main interest was to explore metallo-selectivity in the substitution reaction, we also anticipated that variation of the chalcogen atoms in the cluster amongst the congeners S, Se and Te, could lead to interesting contrasts in the reactivity of the ligand substitution reactions.

Moreover, since the bridged chalcogen atoms form a part of the cluster core, their variation can give rise to interesting changes in the redox behaviour of the clusters. For this purpose we sought to examine changes in redox properties accompanying any structural variations in the cluster system.

We report here the reaction of $[(\eta^5\text{-}C_5H_5)_2Mo_2Fe_2(CO)_7(\mu_3\text{-}E)(\mu_3\text{-}E')]$, $(EE' = Se_2, STe, SeTe, Te_2)$ with isopropyl isocyanide or *tert*-butyl isocyanide, characterisation of the different substituted products, and a study of their electrochemical behaviour.

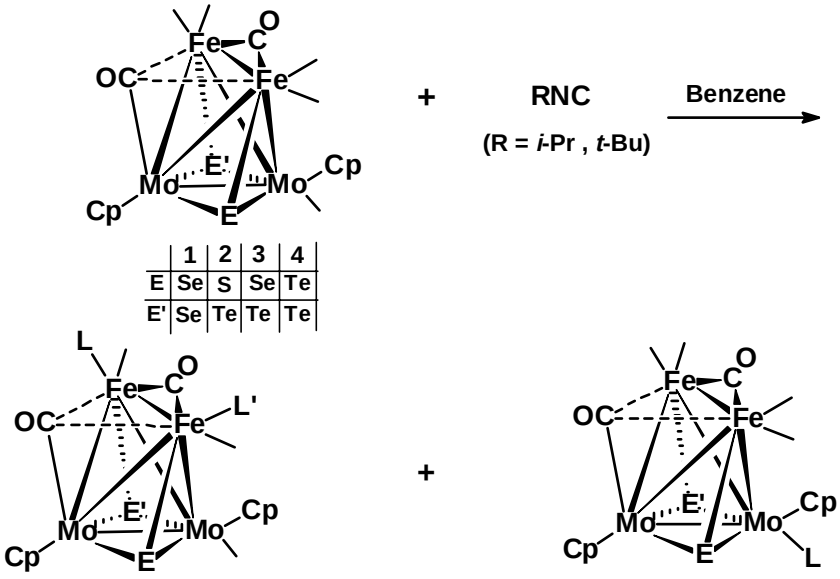

	1	2	3	4
E	Se	S	Se	Te
E'	Se	Te	Te	Te

5 – 12 **13 - 19**

Compd.	E	E'	L	L'
5	Se	Se	^{i}PrNC	CO
6a	S	Te	^{i}PrNC	CO
6b	S	Te	CO	^{i}PrNC
7a	Se	Te	^{i}PrNC	CO
7b	Se	Te	CO	^{i}PrNC
8	Te	Te	^{i}PrNC	CO
9	Se	Se	^{t}BuNC	CO
10a	S	Te	^{t}BuNC	CO
10b	S	Te	CO	^{t}BuNC
11a	Se	Te	^{t}BuNC	CO
11b	Se	Te	CO	^{t}BuNC
12	Te	Te	^{t}BuNC	CO
13	Se	Se	^{i}PrNC	-
14	S	Te	^{i}PrNC	-
15	Se	Te	^{i}PrNC	-
16	Te	Te	^{i}PrNC	-
17	Se	Se	^{t}BuNC	-
18	S	Te	^{t}BuNC	-
19	Se	Te	^{t}BuNC	-

Scheme 1. Reaction of $[Cp_2Mo_2Fe_2(CO)_7(\mu_3\text{-}E)(\mu_3\text{-}E')]$ with RNC.

2. Results and discussion

*2.1. Synthesis and spectroscopic characterisation of [(η^5-C_5H_5)$_2$Mo$_2$Fe$_2$(CO)$_6$(CNR)(μ_3-E)(μ_3-E′)] (**5–19**), (E, E′ = S, Se or Te)*

When a benzene solution of [(η^5-C_5H_5)$_2$Mo$_2$Fe$_2$(CO)$_7$(μ_3-E) (μ_3-E′)] (**1–4**) and isopropyl or *tert*-butyl isocyanide (RNC) was stirred, the isocyanide-substituted derivatives, [(η^5-C_5H_5)$_2$Mo$_2$Fe$_2$ (CO)$_6$(CNR)(μ_3-E)(μ_3-E′)] (**5–19**) were isolated, in yields of 28–62% according to Scheme 1. For all except one E, E′ combination, the substitution occurred at room temperature. Thermolytic conditions were necessary for the reaction of [(η^5-C_5H_5)$_2$Mo$_2$Fe$_2$(CO)$_7$(μ_3-Te)$_2$] (**4**) with Pr^i NC or Bu^{t}NC.

The new compounds were characterised by IR, and by ^{1}H and ^{13}C NMR spectroscopy. Furthermore, the Se- and Te-bridged compounds were characterised by ^{77}Se and ^{125}Te NMR spectroscopy. The ^{77}Se NMR spectra display signals in the range δ 985–1121 ppm, characteristic of μ_3-Se and upfield of signals generally observed for μ_4-Se at $\sim\delta$ 1300 ppm [2,3]. There is a larger variation observed in the ^{125}Te signals, δ 257–1160 ppm, but these fall within the range observed previously for μ_3-Te, and well upfield of signals expected for μ_4-Te, $\sim\delta$ 1600 ppm [3]. The IR spectra of **5–19** show absorptions corresponding to the presence of three types of CO groups: terminal, doubly bridging and semi-triply bridging. The presence of the isocyanide ligand causes a shift to lower frequencies, consistent with substitution of a CO group by a stronger donor but weaker acceptor ligand. The spectra also show the ν_{CN} peak at 2166–2132 cm^{-1}, appropriate for a terminally bonded isocyanide group. For compounds in which the isocyanide ligand is bonded to an iron atom (**5–12**) a single signal was observed in the ^{1}H NMR spectra of the homo-chalcogen derivatives, **5**, **8**, **9** and **12**, whereas the spectra of the mixed-chalcogen species **6**, **7**, **10** and **11**, indicated the presence of two isomers (Scheme 2). Attempts to separate the isomers proved unsuccessful.

In general, upon substitution, the ligand disposition around the metal core remained unchanged in all cases; i.e. five terminal, one doubly bridging and one semi-triply bridging ligand; the isocyanide was found terminally bonded to either of the two Fe atoms, (**5–12**) but only one Mo atom, that was not associated with the semi-triply bridging carbonyl group (**13–19**), consistent with the preference of *i*-PrNC and *t*-BuNC to adopt terminal rather than bridging bonding modes.

Representative single crystal X-ray analyses were carried out on one Fe-substituted product, compound **12**, and one Mo-substituted product, compound **14**. Black crystals of **12** were grown from a hexane/dichloromethane solvent mixture at −5 °C, and its molecular structure is shown in Fig. 1. The metal–metal and metal–tellurium bond distances in **12** are almost identical to those in [(η^5-C_5H_5)$_2$Mo$_2$Fe$_2$(CO)$_7$(μ_3-Te)$_2$] (**12**: Mo–Mo = 2.8886(17) Å; Mo–Fe = 2.908(2) Å, 2.872(2) Å, 2.859(3) Å, 2.855(3) Å; Fe–Fe = 2.417(3) Å; Fe–Te = 2.484(2) Å, 2.478(3) Å ; Mo–Te = 2.7163(19) Å, 2.7041(17) Å, 2.6839(19) Å, 2.6727(17) Å; [(η^5-C_5H_5)$_2$Mo$_2$Fe$_2$(CO)$_7$ (μ_3-Te)$_2$]: Mo–Mo = 2.888(1) Å; Mo–Fe = 2.889(2) Å, 2.872(2) Å, 2.863(2) Å, 2.861(2) Å; Fe–Fe = 2.433(2) Å; Fe–Te = 2.472(2) Å, 2.468(2) Å;

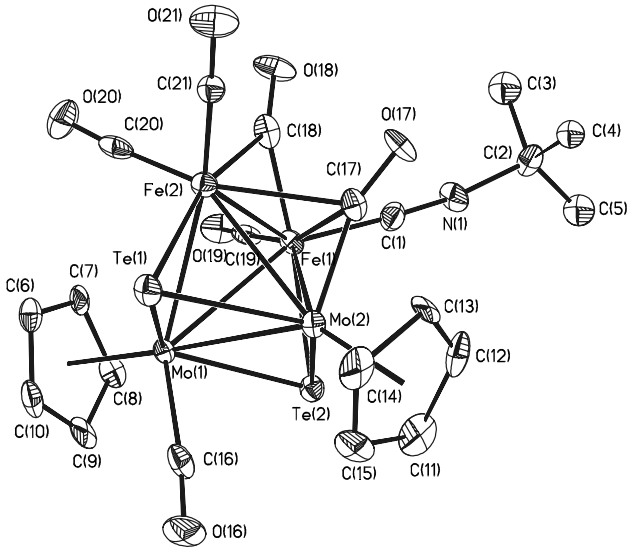

Fig. 1. Molecular structure of [(η^5-C_5H_5)$_2$Mo$_2$Fe$_2${CNC(CH$_3$)$_3$}(CO)$_6$(μ_3-Te)$_2$] (**12**).

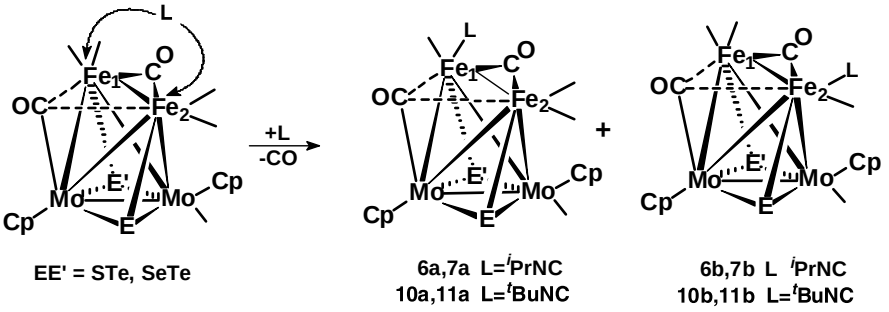

Scheme 2. Formation of two isomers for mixed-chalcogen systems.

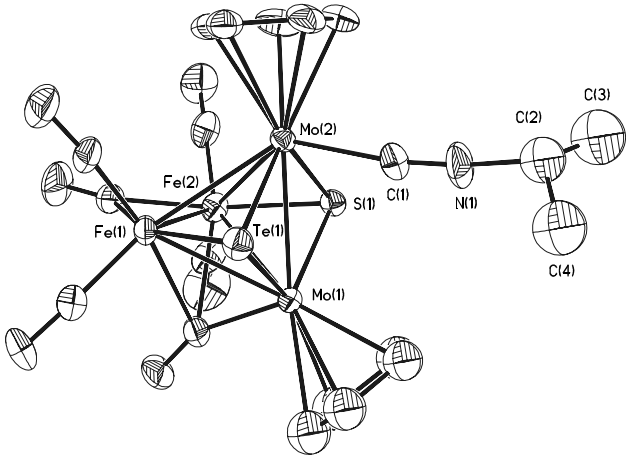

Fig. 2. Molecular structure of $[(\eta^5\text{-}C_5H_5)_2\{(CH_3)_2CHNC\}\{Mo_2Fe_2\}(CO)_6(\mu_3\text{-}S)(\mu_3\text{-}Te)]$ (**14**).

Mo–Te = 2.684(1) Å, 2.683(1) Å, 2.681(1) Å, 2.673(1) Å).[4] The C–N bond distance of 1.164(16) Å in **12** is comparable to the C–N bond distances of the linear $CNBu^t$ groups in $[Fe(CNBu^t)_5]$ (1.16(1)–1.19(1) Å) [8].

Green crystals of compound **14** were obtained from a hexane/dichloromethane solvent mixture at −5 °C. Its molecular structure, shown in Fig. 2 confirms that here too the metal core remains unchanged upon isocyanide substitution. One of the molybdenum atoms has a terminally bonded isopropyl isocyanide group. The C–N distance of 1.157(11) Å in **14** is comparable to that observed for the terminal $CNPr^i$ ligand in $[Mo(CO_2)_2(PMe_3)_3(CNPr^i)]$ (1.14(3) Å) [9].

2.2. Redox properties of compounds *2, 6, 8, 12* and *14*

The redox properties of complexes **2**, **6**, **8**, **12** and **14** (Fig. 3) have been studied in dichloromethane solvent by cyclic voltammetry in the potential range ±2.5 V at 298 K, using a platinum working electrode. The voltammograms are shown in Fig. 4(a–e).

Complex **2** displays one irreversible oxidative response *E*pa, at 1.0 V and one irreversible reduction *E*pc, at −1.07 V vs. SCE (Fig. 4a). Similarly, complex **14** exhibits both irreversible oxidative (*E*pa) and reductive (*E*pc) responses at 1.0 and −1.35 V vs. SCE, respectively (Fig. 4c). However, in the case of **6**, two closely spaced irreversible oxidative responses (E^1pa, 0.77 V and E^2pa, 0.99 V; ΔEpa = 220 mV) and two successive quasi-reversible reductions [E°_{298}, V(ΔEp, mV), −0.91 (90) and −1.29 (120)] (Fig. 4b) have been observed.

Comparison of the redox behaviour of **2** and **14** reveals that, as anticipated from the replacement of a carbonyl ligand on molybdenum by the better donor isonitrile ligand, the more electron-rich cluster is more difficult to reduce. The ^{1}H NMR spectrum of **6** in $CDCl_3$ indicates the presence of an inseparable mixture of two diastereomers, one with Fe1–CN^iPr where Fe1 is bonded to μ_3-S in the cluster core and the other with

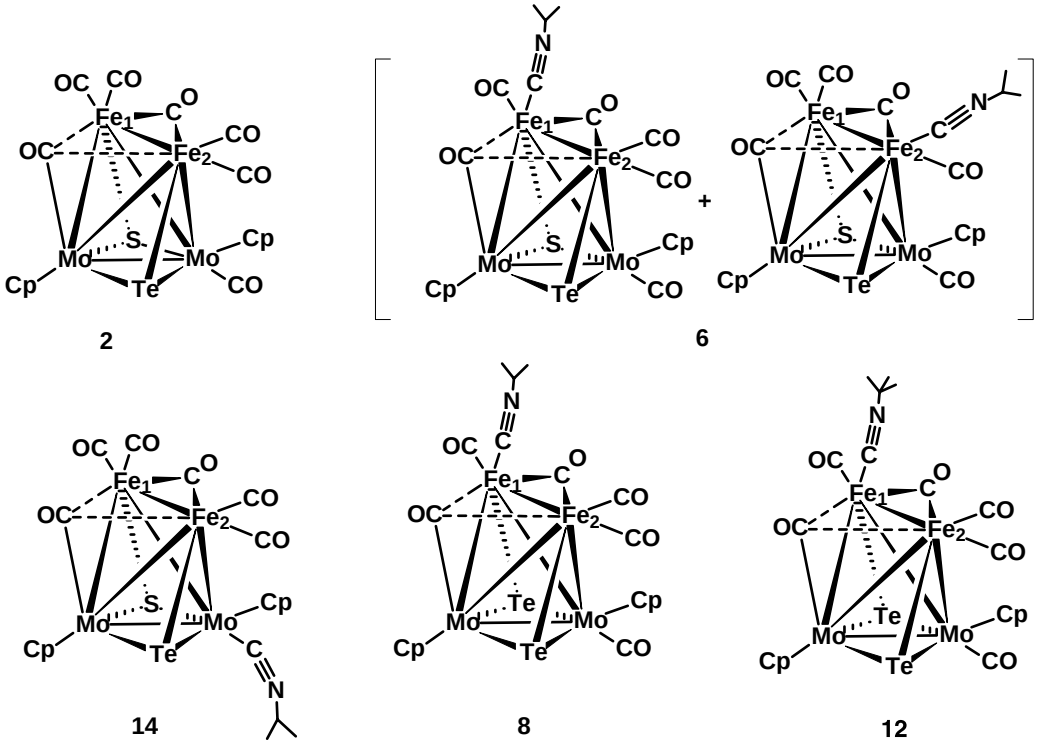

Fig. 3. Structures of compounds **2**, **6**, **8**, **12** and **14**.

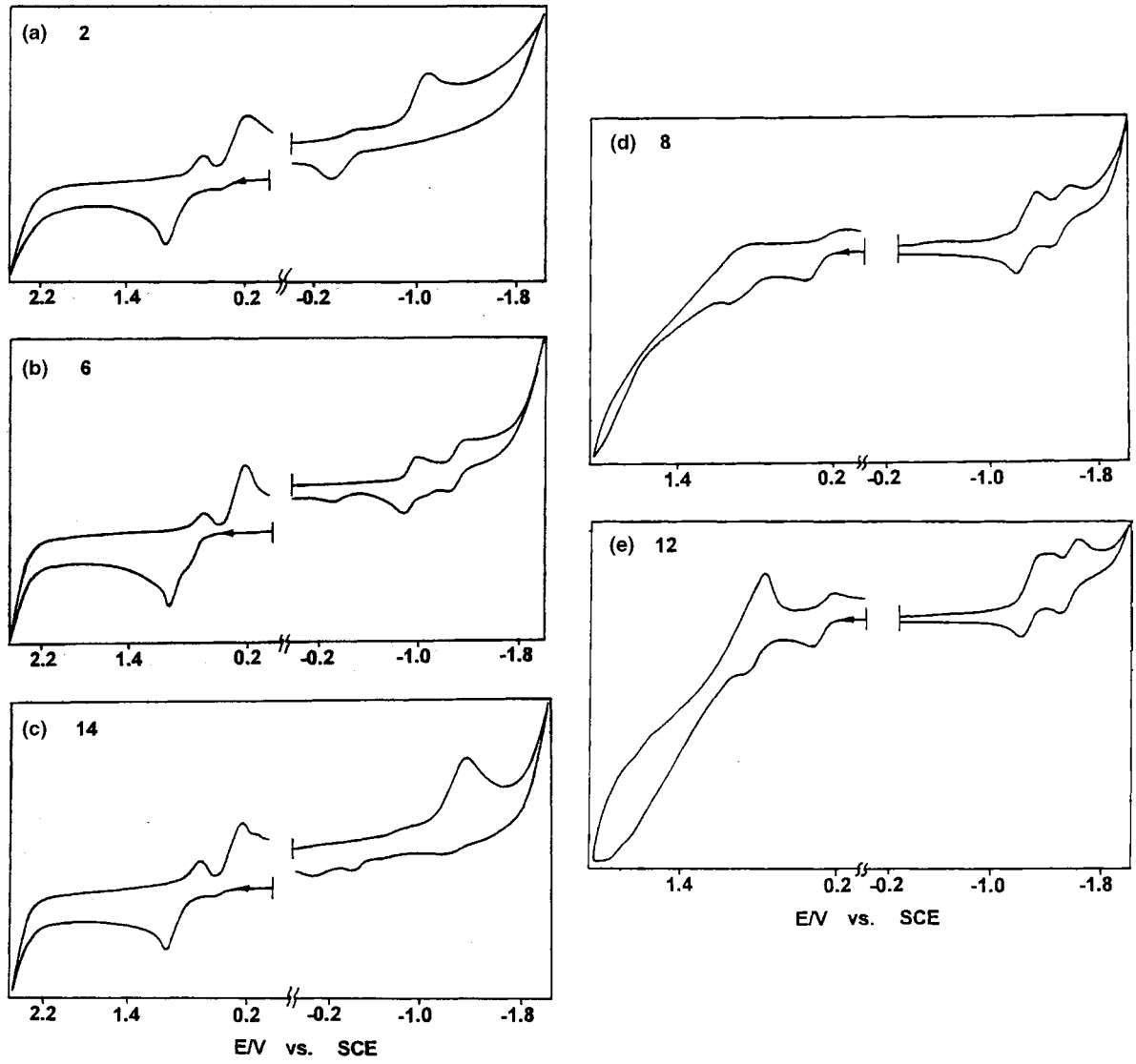

Fig. 4. (a–c) Cyclic voltammograms of **2**, **6** and **14** (d–e) Cyclic voltammograms of **8** and **12**.

Fe2–CN^{i}Pr where Fe2 is bonded to μ_3-Te in the cluster core, and this may account for the observation of two oxidative and two reductive responses in **6** (Fig. 4b). In contrast, we note that only a single isomer of **14**, is produced, and this gives rise to only one oxidation and one reduction process.

The splitting of the anodic waves in Fig. 4b is observed to be enhanced appreciably in case of **8** with two oxidative responses at E^1pa, 0.384 V and E^2pa, 0.933 V (ΔEp = 549 mV) and two reductive responses $E°_{298}$, V (ΔEp, mV) at −1.28 (150) and −1.52 (130) (Fig. 4d). Similarly, **12** exhibits oxidative responses at E^1pa, 0.37 V and E^2pa, 0.89 V (ΔEpa = 520 mV) and reductive responses $E°_{298}$, V (ΔEp, mV) at −1.30 (180) and −1.57 (130) (Fig. 4e). The larger splitting in **8** (ΔEpa = 540 mV) and **12** (ΔEpa = 520 mV) compared to **6** (ΔEpa = 220 mV) is possibly attributable to the presence of different chalcogen combinations in the cluster cores. The presence of a $(\mu_3\text{-Te})_2$ unit in the cluster core of **8** and **12** increases the electron density at the iron centres relative to that of **6**, where (μ_3-S)(μ_3-Te) is present which in turn decreases the potentials as expected. Moreover, the decrease in anodic potentials and increase in cathodic potentials in **12** as compared to **8** is rationalisable in terms of the replacement of an isopropyl isocyanide group by the more electron-donating *t*-butyl isocyanide group.

3. Experimental section

3.1. General procedures

All reactions and other manipulations were carried out using standard Schlenk techniques under an inert atmosphere of argon. All solvents were deoxygenated immediately prior to use. Infrared spectra were recorded on a Nicolet Impact 400 FTIR spectrophotometer, as *n*-

Table 1
Experimental conditions for the preparation of **5**–**19**

Reactants/mg (mmol)	Reaction conditions (Time, temperature)	Compound	Yield mg (%)	Analysis (%) Calculated (Found)	mp/°C[a]
$[Cp_2Mo_2Fe_2Se_2(CO)_7]$ + $[(CH_3)_2CHCN]$ 100 (0.13) 15 μlt (0.17)	10 h, 25 °C	**5**	30 (28)	C, 28.96 (28.44); H, 2.05 (2.57); N 1.69 (1.78)	130–132
		13	63 (59)	C, 28.96 (28.35); H, 2.05 (2.17); N 1.69 (1.72)	134–135
$[Cp_2Mo_2Fe_2STe(CO)_7]$ + $[(CH_3)_2CHCN]$ 100 (0.13) 15 μlt (0.17)	12 h, 25 °C	**6a + 6b**	52 (48)	C, 28.8 (28.22); H, 2.04 (2.19); N 1.68 (1.71)	131–134
		14	31 (29)	C, 28.8 (28.46); H, 2.04 (2.12); N 1.68 (1.72)	140–142
$[Cp_2Mo_2Fe_2SeTe(CO)_7]$ + $[(CH_3)_2CHCN]$ 100 (0.12) 15 μlt (0.17)	20 h, 25 °C	**7a + 7b**	40 (38)	C, 27.35 (27.00); H, 1.94 (2.18); N 1.59 (1.65)	141–143
		15	37 (35)	C, 27.35 (26.95); H, 1.94 (2.30); N 1.59 (1.64)	148–150
$[Cp_2Mo_2Fe_2Te_2(CO)_7]$ + $[(CH_3)_2CHCN]$ 100 (0.11) 15 μlt (0.17)	20 h, 60 °C	**8**	35 (34)	C, 25.92 (25.85); H, 1.84 (2.21); N, 1.47 (1.50)	145–147
		16	26 (25.5)	C, 25.92 (25.56); H, 1.84 (2.16); N, 1.47 (1.53)	153–154
$[Cp_2Mo_2Fe_2Se_2(CO)_7]$ + $[(CH_3)_3CCN]$ 100 (0.13) 20 μlt (0.18)	10 h, 25 °C	**9**	34 (31)	C, 29.98 (29.6); H, 2.26 (2.51); N, 1.66 (1.68)	136–137
		17	60 (55)	C, 29.98 (29.3); H, 2.26 (2.47); N, 1.66 (1.73)	140–142
$[Cp_2Mo_2Fe_2STe(CO)_7]$ + $[(CH_3)_3CCN]$ 100 (0.13) 20 μlt (0.18)	12 h, 25 °C	**10a + 10b**	49 (45)	C, 29.91 (29.64); H, 2.26 (2.31); N, 1.66 (1.69)	141–142
		18	33 (30)	C, 29.91 (29.53); H, 2.26 (2.45); N, 1.66 (1.72)	146–148
$[Cp_2Mo_2Fe_2SeTe(CO)_7]$ + $[(CH_3)_3CCN]$ 100 (0.12) 20 μlt (0.18)	20 h, 25 °C	**11a + 11b**	45 (42)	C, 28.3 (27.85); H, 2.15 (2.24); N 1.57 (1.68)	155–157
		19	36 (34)	C, 28.3 (27.75); H, 2.15 (2.34); N 1.57 (1.61)	147–149
$[Cp_2Mo_2Fe_2Te_2(CO)_7]$ + $[(CH_3)_3CCN]$ 100 (0.11) 20 μlt (0.18)	20 h, 60 °C	**12**	65 (62)	C, 26.9 (26.26); H, 2.04 (2.29); N 1.5 (1.64)	140–141

[a] With decomposition.

hexane solutions in 0.1 mm path length cells. Elemental analyses were performed using a Carlo-Erba automatic analyser. ^{1}H, ^{13}C, ^{77}Se, ^{125}Te NMR spectra were recorded on a Varian VXR-300S spectrometer in $CDCl_3$. The operating frequency for ^{125}Te was 94.70 MHz with a pulse width of 9.5 μs and a delay of 1.0 s. ^{125}Te NMR spectra were referenced to Me_2Te ($\delta = 0$ ppm). The ^{77}Se NMR measurements were made at an operating frequency of 57.23 MHz using 90° pulses with a 1.0 s delay and 1.0 s acquisition time and referenced to Me_2Se ($\delta = 0$). Electrochemical measurements were carried out using a PAR model 273 A potentiostat/galvanostat. A platinum working electrode, a platinum auxiliary electrode and a saturated calomel reference electrode (SCE) were used in a three-electrode configuration. Tetraethyl ammonium perchlorate (TEAP) was the supporting electrolyte, and the solute concentration was $\sim 10^{-3}$ M. The half-wave potential $E°_{298}$ was set equal to 0.5 (Epa + Epc), where Epa and Epc are the anodic and cathodic cyclic voltammetric peak potentials, respectively. For irreversible processes Epa and Epc are considered. It should be noted that while doing the cyclic voltammetric experiments we encountered electrode poisoning. Therefore, the electrodes were treated with acid-water and dried prior to each scan. Electronic spectra were recorded using a Shimadzu UV-2100 spectrophotometer.

The starting materials $[Cp_2Mo_2Fe_2(CO)_7(\mu_3\text{-}E)(\mu_3\text{-}E')]$ (where $EE' = Se_2$, STe, Te_2, SeTe) were prepared as reported in literature [1–4]. Details of the quantities of

Table 2
Spectral data for compound **5**–**19**

Compound	I.R. (ν) (cm^{-1})	^{1}H NMR (δ)	^{13}C NMR (δ)	^{77}Se NMR	^{125}Te NMR
5	[a]2145.2(m), 2133.1(m), 2001.3(s), 1955.4(s), 1944.8(vs), 1847.3(m, br), 1740(w) [b]1991.9(s), 1958.9(vs, br), 1828.2(m, br), 1735(w)	5.4, 5.09(C_5H_5), 4.31(m, CH), 1.31(dd, CH_3,)	93.56, 91.05(C_5H_5), 23.29(CH_3), 44.5 (CH), 137.1(CN), 210, 214(CO)	1050.6, 985.5	–
6a	[a]2143.2(w), 2132.7(w), 2000.8(vs), 1953.1(s), 1940.4(vs), 1843.7(m, br), 1742.0(w)	5.39, 5.08(C_5H_5), 3.87(m, CH), 1.32(t, CH_3)	93.83, 91.22(C_5H_5), 23.67(CH_3), 53.5(CH), 135.35(CN), 215, 213(CO)	–	1160.4, 1129
6b	[b]1991.8(s), 1953.4(vs, br), 1818(m, br), 1737(w)	5.40, 5.09(C_5H_5), 4.07(m, CH), 1.44(dd, CH_3)			
7a	[a]2142(w), 2135.3(w), 2000.8(vs), 1951.2(vs), 1933.1(vs), 1839.2(m, br), 1736.6(w)	5.34, 5.05(C_5H_5), 3.87(m, CH), 1.32(t, CH_3)	93.14, 90.79(C_5H_5), 19.3(CH_3), 41.93(CH), 163.2(CN), 200, 204(CO)	1086.3	365.8, 500.4
7b	[b]2127(m, br), 1988.3(s), 1939(vs, br), 1813(m, br), 1735.2(w).	5.35, 5.053(C_5H_5), 4.06(m, CH), 1.42(t, CH_3)			
8	[a]2144(w), 2132(w), 1997.4(vs), 1947.6(vs), 1923(vs), 1830(m, br), 1737(w) [b]2125.4(m), 1986.4(vs), 1936.0(vs), 1927.6(vs), 1812.5(m, br), 1734(w).	5.3, 5.01(C_5H_5), 3.88(m, CH), 1.307(t, CH_3)	91.93, 89.94(C_5H_5), 23.89(CH_3), 41.2(CH), 164.1(CN), 213, 216(CO)	–	328, 462.3
9	[a]2001.2(s), 1956.7(s), 1945(vs), 1847(m), 1741(w) [b]2055(m), 1992.3(s), 1958(vs, br), 1818.6(m), 1737(w)	5.39, 5.09(C_5H_5), 1.38(s, CH_3)	93.65, 90.23(C_5H_5), 30.02(CH_3), 53.8(C), 166.5(CN), 212, 216(CO)	1065.6, 1108.4	–
10a	[a]2133(w, br), 1999.4(s), 1951.4(s), 1941.9(vs), 1842.1(w, br), 1741.7(w)	5.48, 5.17(C_5H_5), 1.38(s, CH_3)	93.5, 90.8(C_5H_5), 29.7(CH_3), 55.4(C), 161(CN), 210, 208(CO)	–	1056, 1084.7
10b	[b]1989.1(s), 1949(br, vs), 1819.9(m, br),	5.30, 5.09(C_5H_5), 1.38(s, CH_3)			
11a	[a]2136(m, br), 1999.3(vs), 1950(vs), 1935(vs), 1837(w, br), 1743(w)	5.34, 5.05(C_5H_5), 1.38(s, CH_3)	92.9, 90.0(C_5H_5), 29.4(CH_3), 55.2(C), 162(CN), 214, 210(CO)	1025.2, 1121.6	257.3, 405.3
11b	[b]1987.7(s), 1942.1(vs, br), 1819.1(m, br), 1751.7(w)	5.338, 5.046(C_5H_5), 1.38(s, CH_3)			

12	[a]2135(m, br), 2000(vs), 1948.5(vs), 1919(vs), 1833.8(w), 1736(w) [b]1985.9(vs), 1934(vs, br), 1815.6(w, br).	5.29, 5.01(C_5H_5), 1.36(s, CH_3)	91.3, 89.5(C_5H_5), 30.1(CH_3), 54.2(C), 167.3(CN), 211, 214(CO)	–	330, 396.5
13	[a]2157(m, br), 2014(s), 1997.3(s), 1820(w, br), 1744(w) [b]2003.6(vs), 1976.5(vs), 1941.8(s), 1813(w), 1733(w)	5.41, 5.07(C_5H_5), 4.07(m, CH), 1.43(d, CH_3)	92.6, 90.58(C_5H_5), 23.05(CH_3), 44.82(CH), 136.3(CN), 215, 213(CO)	1110.0	–
14	[a]2166.4(w),2137(w), 2012.4(s), 1991.6(s), 1950(s), 1839(w, br), 1736(w) [b]2002(vs), 1975.3(vs), 1940.6(s), 1813(w, br), 1750(w)	5.40, 5.06(C_5H_5), 4.04(m, CH), 1.405(dd, CH_3)	92.2, 90.6(C_5H_5), 23.2 (CH_3), 43.5(CH), 133.2(CN), 211, 214(CO)	–	814.6
15	[a]2157.8(w), 2137(w), 2013.4(s), 1989.4(s), 1953(vs), 1835(w, br), 1742(w) [b]2002.6(vs), 1975.2(vs), 1941(s), 1820.7(m, br), 1754.8(w).	5.35, 5.01(C_5H_5), 4.06(m, CH), 1.38(dd, CH_3)	91.92, 90.35(C_5H_5), 23.62(CH_3), 42.8(CH), 133.67(CN)	1098.6	560.8
16	[a]2155.6(w), 2134(w), 2015(s), 1989.0(s), 1955(vs), 1840(w, br), 1743(w) [b]2004.0(vs), 1974.5(vs), 1940.7(s), 1819.3(m), 1752.4(w)	5.3, 4.96(C_5H_5), 3.99(m, CH), 1.33(dd, CH_3)	91.05, 89.81(C_5H_5), 23.39(CH_3), 48.3(CH), 129.6(CN), 213, 211	–	478.3
17	[a]2153.2(w), 2137(w), 2013.1(s), 1990.5(s), 1953.2(s), 1838(w, br), 1739.6(w) [b]2002.5(vs), 1974.2(vs), 1942.8(m), 1813.2(w), 1743(w)	5.41, 5.07(C_5H_5), 1.5(s, CH_3)	92.38, 90.55(C_5H_5), 28.6(CH_3), 55.3(C), 164.5(CN), 214, 209	1104.8	–
18	[a]2154(w), 2139(w), 2013(s), 1988.9(vs), 1953(vs), 1836.7(m, br), 1743(w) [b]2001.6(vs), 1973.3(vs), 1943(m, br), 1814.2(w), 1741(w)	5.40, 5.05(C_5H_5), 1.46(s, CH_3)	92.7, 90.4(C_5H_5), 29.5(CH_3), 55.6(C), 166(CN), 211, 215(CO)	–	839.0
19	[a]2157(w), 2138.2(w), 2012(vs), 1989(s), 1950(vs), 1834(w), 1742(w). [b]2002.3(vs), 1974(vs), 1942(s), 1819(m, br), 1753(w).	5.35, 5.01(C_5H_5), 1.44(s, CH_3)	91.83, 90.16(C_5H_5), 30.48(CH_3), 53.4(C), 162.8(CN), 210, 216	1116.2	680.2

[a] *n*-hexane.
[b] CH_2Cl_2.

Table 3
Crystal data and structure refinement for 12 and 14

Identification code	**12**	**14**
Empirical formula	$C_{21}H_{19}Fe_2Mo_2N\ O_6Te_2$	$C_{20}H_{17}\ Fe_2Mo_2N\ O_6S\ Te$
Formula weight	940.15	830.59
Temperature	299(2) K	299(2) K
Wavelength	0.71073 Å	0.71073 Å
Crystal system	Monoclinic	Monoclinic
Space group	C2/c	P2(1)/c
a, Å	16.615(6)	14.325(7)
b, Å	10.507(4)	12.315(6)
c, Å	29.659(11)	15.775(9)
β, degree	98.987(7)	116.364(9)
Volume	5114 (3) Å^3	2493(2) Å^3
Z	8	4
Density (calculated)	2.442 Mg/m^3	2.213 Mg/m^3
Absorption coefficient	4.344 mm^{-1}	3.389 mm^{-1}
F(0 0 0)	3520	1584
Crystal size	$0.05 \times 0.08 \times 0.12$ mm^3	$0.5 \times 0.3 \times 0.1$ mm^3
θ range for data collection	1.39° to 22.50°.	1.59° to 25.00°
Index ranges	$-17 \leqslant h \leqslant 17$, $-11 \leqslant k \leqslant 11$, $-31 \leqslant l \leqslant 31$	$-17 \leqslant h \leqslant 17$, $-14 \leqslant k \leqslant 14$, $-18 \leqslant l \leqslant 18$
Reflections collected	15,314	18,485
Independent reflections	3346 [$R(int) = 0.1383$]	4375 [$R(int) = 0.0386$]
Refinement method	Full-matrix least-squares on F^2	Full-matrix least-squares on F^2
Data/restraints/parameters	3346/0/288	4375/0/259
Goodness-of-fit on F^2	0.978	1.037
Final *R* indices [I>2σ(I)]	$R1 = 0.0522$, $wR2 = 0.0890$	$R1 = 0.0473$, $wR2 = 0.1246$
R indices (all data)	$R1 = 0.1173$, $wR2 = 0.1070$	$R1 = 0.0646$, $wR2 = 0.1357$
Largest different peak and hole	1.250 and −1.015 e.Å^{-3}	2.492 and −0.918 e.Å^{-3}
Ratio of min to max apparent transmission	0.740012	0.551528

starting materials used and the yields of products obtained are given in Table 1. See Table 2 for spectral data.

3.2. Reaction of $[Cp_2Mo_2Fe_2(CO)_7(\mu_3\text{-}E)(\mu_3\text{-}E')]$ (E, E′ = S, S; S, Te; Se, Te; Te, Te) with RNC [R = ^{i}Pr or ^{t}Bu]

A benzene solution of $[Cp_2Mo_2Fe_2(CO)_7(\mu_3\text{-}E)(\mu_3\text{-}E')]$ was stirred with RNC (R = $(CH_3)_2CH$ or $(CH_3)_3C$) at room temperature for the chalcogen combination EE′ = Se_2, STe and SeTe and at 60 °C for EE′ = Te_2. The reaction was monitored using thin layer chromatography. After completion of the reaction, the solution was filtered to remove any insoluble material and the solvent was removed from the filtrate. The residue was dissolved in dichloromethane and chromatographic work-up was performed. Using (30/70 v/v) *n*-hexane-dichloromethane solvent mixtures as eluent, two fractions were isolated. The first fraction was a black compound which was shown to bear an isocyanide ligand at an iron centre, $[Cp_2Mo_2Fe_2(RNC)(CO)_6(\mu_3\text{-}E)(\mu_3\text{-}E')]$, [E = E′ = Se, R = $(CH_2)_2CH$ (**5**) or $(CH_3)_3C$ (**9**); E = E′ = Te, R = $(CH_3)_2CH$ (**8**) or $(CH_3)_3C$ (**12**); E = S, E′ = Te, R = $(CH_3)_2CH$ (**6a**, **6b**) or R = $(CH_3)_3C$ (**10a**, **10b**); E = Se, E′ = Te, R = $(CH_3)_2CH$ (**7a**, **7b**) or R = $(CH_3)_3C$ (**11a**, **11b**)] For mixed-chalcogen combinations two isomers of the iron-monosubstituted isocyanide complexes were identified by NMR spectroscopy, but could not be separated by TLC. The second fraction was characterised as a green compound in which substitution had occurred at a molybdenum centre, $[Cp_2(RNC)Mo_2Fe_2(CO)_6(\mu_3\text{-}E)(\mu_3\text{-}E')]$, [E = E′ = Se, R = $(CH_3)_2CH$ (**13**) or $(CH_3)_3C$ (**17**); E = E′ = Te, R = $(CH_3)_2CH$ (**16**) ; E = S, E′ = Te, R = $(CH_3)_2CH$ (**14**) or R = $(CH_3)_3C$, (**18**); E = Se, E′ = Te, R = $(CH_3)_2CH$ (**15**) or R = $(CH_3)_3C$ (**19**)]. UV data: **2**, (dichloromethane; λ_{max}, nm (ε, M^{-1} cm^{-1}): 596 (1710), 506 (3220), 382 (7920), 295 (28,190), 233 (64,220); **6**, (dichloromethane; λ_{max}, nm (ε, M^{-1} cm^{-1}): 594 (1930), 484 (3334), 381 (8190), 294 (28,045), 232 (65,682); **8**, (dichloromethane; λ_{max}, nm (ε, M^{-1} cm^{-1}): 600 (1915), 475 (3542), 374 (7589), 303 (27,865), 234 (66,721); **12**, (dichloromethane; λ_{max}, nm (ε, M^{-1} cm^{-1}): 590 (1920), 482 (3289), 378 (9682), 288 (26,531), 235 (65,890); **14**, (dichloromethane; λ_{max}, nm (ε, M^{-1} cm^{-1}): 606 (1246), 472 (2013), 371 (5530), 286 (21,883), 231 (47,344).

3.3. Crystal structure determination of 12 and 14

Crystals of compounds **12** and **14** suitable for X-ray diffraction analysis were grown from hexane-dichloromethane solvent mixtures by slow evaporation of the solvents at −5 °C. Relevant crystallographic data and details of measurements are given in Table 3. Selected

Table 4
Selected bond lengths [Å] and angles [°] for 12

Mo(1)–Te(2)	2.6727(17)	Fe(1)–C(1)	1.852(17)
Mo(1)–Te(1)	2.6839(19)	Fe(1)–C(18)	1.891(18)
Mo(1)–Fe(2)	2.859(3)	Fe(1)–Fe(2)	2.417(3)
Mo(1)–Mo(2)	2.8886(17)	Fe(1)–Te(2)	2.478(3)
Mo(1)–Fe(1)	2.908(2)	Fe(2)–C(18)	2.010(16)
Mo(2)–C(17)	1.981(17)	Fe(2)–Te(1)	2.484(2)
Mo(2)–Te(1)	2.7041(17)	C(1)–N(1)	1.164(16)
Mo(2)–Te(2)	2.7163(19)	N(1)–C(2)	1.478(19)
Mo(2)–Fe(1)	2.855(3)	O(17)–C(17)	1.174(16)
Mo(2)–Fe(2)	2.872(2)	O(18)–C(18)	1.171(17)
Te(2)–Mo(1)–Te(1)	116.15(6)	Te(2)–Fe(1)–Mo(2)	60.76(6)
Te(2)–Mo(1)–Fe(2)	96.41(6)	Fe(2)–Fe(1)–Mo(1)	65.40(8)
Te(1)–Mo(1)–Fe(2)	53.13(5)	Te(2)–Fe(1)–Mo(1)	58.86(6)
Te(2)–Mo(1)–Mo(2)	58.32(5)	Mo(2)–Fe(1)–Mo(1)	60.16(6)
Te(1)–Mo(1)–Mo(2)	57.92(4)	Fe(1)–Fe(2)–Te(1)	115.86(10)
Fe(2)–Mo(1)–Mo(2)	59.94(5)	Fe(1)–Fe(2)–Mo(1)	66.28(7)
Te(2)–Mo(1)–Fe(1)	52.50(5)	Te(1)–Fe(2)–Mo(1)	59.81(6)
Te(1)–Mo(1)–Fe(1)	95.83(6)	Fe(1)–Fe(2)–Mo(2)	64.68(7)
Fe(2)–Mo(1)–Fe(1)	49.53(7)	Te(1)–Fe(2)–Mo(2)	60.14(6)
Mo(2)–Mo(1)–Fe(1)	59.01(5)	Mo(1)–Fe(2)–Mo(2)	60.54(6)
Te(1)–Mo(2)–Te(2)	114.02(5)	Fe(2)–Te(1)–Mo(1)	67.07(7)
Te(1)–Mo(2)–Fe(1)	96.64(6)	Fe(2)–Te(1)–Mo(2)	67.06(6)
Te(2)–Mo(2)–Fe(1)	52.75(6)	Mo(1)–Te(1)–Mo(2)	64.84(5)
Te(1)–Mo(2)–Fe(2)	52.80(5)	Fe(1)–Te(2)–Mo(1)	68.62(6)
Te(2)–Mo(2)–Fe(2)	95.16(6)	Fe(1)–Te(2)–Mo(2)	66.49(6)
Fe(1)–Mo(2)–Fe(2)	49.92(6)	Mo(1)–Te(2)–Mo(2)	64.82(5)
Te(1)–Mo(2)–Mo(1)	57.24(4)	N(1)–C(1)–Fe(1)	176.0(15)
Te(2)–Mo(2)–Mo(1)	56.84(6)	C(1)–N(1)–C(2)	167.0(16)
Fe(1)–Mo(2)–Mo(1)	60.83(5)	O(17)–C(17)–Mo(2)	155.3(12)
Fe(2)–Mo(2)–Mo(1)	59.53(5)	O(17)–C(17)–Fe(2)	120.7(11)
C(1)–Fe(1)–Fe(2)	130.6(5)	O(17)–C(17)–Fe(1)	120.5(11)
Fe(2)–Fe(1)–Te(2)	114.92(10)	O(18)–C(18)–Fe(1)	146.2(14)
C(1)–Fe(1)–Mo(2)	104.6(5)	O(18)–C(18)–Fe(2)	137.3(14)
Fe(2)–Fe(1)–Mo(2)	65.40(8)		

bond lengths and bond angles for **12** and **14** are given in Tables 4 and 5, respectively. X-ray crystallographic data were collected from single crystal samples of **12** ($0.12 \times 0.08 \times 0.05$ mm^3), and **14** ($0.50 \times 0.30 \times 0.10$ mm^3), mounted on glass fibres. Data were collected using a P4 Bruker diffractometer, equipped with a Bruker SMART 1 K charge coupled device (CCD) area detector, using the program SMART [10], and a rotating anode, using graphite-monochromated Mo K_α radiation ($\lambda = 0.71073$ Å). The crystal-to-detector distance was 4.987 cm, and the data collection was carried out in 512×512 pixel mode, utilising 2×2 pixel binning. The initial unit cell parameters were determined by a least-squares fit of the angular settings of the strong reflections, collected by a 12° scan in 40 frames over three different sections of reciprocal space (120 frames in total). A complete sphere of data was collected, to better than 0.8 Å resolution at 298 K. Upon completion of the data collection, the first 50 frames were recollected in order to improve the decay correction analyses. Processing was carried out using the program SAINT [11], which applied Lorentz and polarisation corrections to the three-dimensionally integrated diffraction spots. The program SADABS [12], was utilised for the scaling of diffraction data, the application of a decay correction, and an empirical absorption correction based on redundant reflections for all data sets. The structures were solved by using the direct-methods procedure in the Bruker SHELXTL program library [13], and refined by full-matrix least squares methods on F^2 with anisotropic thermal parameters for all non-hydrogen atoms with the exception of the isopropyl moiety and one Cp ring in **14**, and three methyl carbons within the *t*-butyl group of **12**. The *tert*-butyl amine moiety in **12** contained a slight rotational disorder, which could not be modelled effectively and therefore required anisotropic refinement of these carbons. The disorder of the Cp ring in **14** was not resolvable. The molecular packing illustrated that this disorder contributed directly to a positional disorder of the isopropyl group, which was also refined isotropically. Hydrogen atoms were added as fixed contributors at calculated positions, with isotropic thermal parameters based on the carbon atom to which they were bonded.

Table 5
Selected bond lengths [Å] and bond angles [°] for 14

Mo(1)–C(15)	1.964(9)	Fe(1)–C(15)	2.375(10)
Mo(1)–S(1)	2.373(2)	Fe(1)–Fe(2)	2.488(2)
Mo(1)–Te(1)	2.6700(13)	Fe(1)–Te(1)	2.4923(16)
Mo(1)–Fe(2)	2.7658(16)	Fe(2)–C(16)	1.963(9)
Mo(1)–Fe(1)	2.8166(16)	Fe(2)–S(1)	2.214(2)
Mo(1)–Mo(2)	2.8394(18)	Fe(2)–C(15)	2.444(10)
Mo(2)–C(1)	2.088(9)	N(1)–C(1)	1.157(11)
Mo(2)–S(1)	2.368(2)	N(1)–C(2)	1.457(16)
Mo(2)–Te(1)	2.6552(14)	C(2)–C(3)	1.44(2)
Mo(2)–Fe(2)	2.8050(16)	C(2)–C(4)	1.47(2)
Mo(2)–Fe(1)	2.8432(16)	O(15)–C(15)	1.180(11)
Fe(1)–C(16)	1.941(9)	O(16)–C(16)	1.151(10)
C(15)–Mo(1)–S(1)	105.2(3)	Te(1)–Mo(2)–Fe(1)	53.78(4)
C(15)–Mo(1)–Te(1)	101.9(3)	Fe(2)–Mo(2)–Fe(1)	52.28(5)
S(1)–Mo(1)–Te(1)	110.39(7)	Mo(1)–Mo(2)–Fe(1)	59.43(3)
C(15)–Mo(1)–Fe(2)	59.4(3)	Fe(2)–Fe(1)–Te(1)	112.32(5)
S(1)–Mo(1)–Fe(2)	50.33(6)	Fe(2)–Fe(1)–Mo(1)	62.48(4)
Te(1)–Mo(1)–Fe(2)	99.10(5)	Te(1)–Fe(1)–Mo(1)	60.02(4)
C(15)–Mo(1)–Fe(1)	56.2(3)	Fe(2)–Fe(1)–Mo(2)	63.07(4)
S(1)–Mo(1)–Fe(1)	94.44(7)	Te(1)–Fe(1)–Mo(2)	59.26(4)
Te(1)–Mo(1)–Fe(1)	53.95(4)	Mo(1)–Fe(1)–Mo(2)	60.22(4)
Fe(2)–Mo(1)–Fe(1)	52.94(5)	S(1)–Fe(2)–Fe(1)	108.54(7)
C(15)–Mo(1)–Mo(2)	109.7(3)	S(1)–Fe(2)–Mo(1)	55.59(6)
S(1)–Mo(1)–Mo(2)	53.13(6)	Fe(1)–Fe(2)–Mo(1)	64.58(5)
Te(1)–Mo(1)–Mo(2)	57.53(4)	S(1)–Fe(2)–Mo(2)	54.78(7)
Fe(2)–Mo(1)–Mo(2)	60.04(4)	Fe(1)–Fe(2)–Mo(2)	64.65(4)
Fe(1)–Mo(1)–Mo(2)	60.35(4)	Mo(1)–Fe(2)–Mo(2)	61.28(4)
C(1)–Mo(2)–S(1)	83.4(3)	Fe(1)–Te(1)–Mo(2)	66.97(4)
C(1)–Mo(2)–Te(1)	80.7(3)	Fe(1)–Te(1)–Mo(1)	66.03(4)
S(1)–Mo(2)–Te(1)	111.05(7)	Mo(2)–Te(1)–Mo(1)	64.44(5)
C(1)–Mo(2)–Fe(2)	129.9(3)	Fe(2)–S(1)–Mo(2)	75.41(7)
S(1)–Mo(2)–Fe(2)	49.80(5)	Fe(2)–S(1)–Mo(1)	74.08(7)
Te(1)–Mo(2)–Fe(2)	98.48(4)	Mo(2)–S(1)–Mo(1)	73.59(8)
C(1)–Mo(2)–Mo(1)	80.6(3)	C(1)–N(1)–C(2)	171.9(13)
S(1)–Mo(2)–Mo(1)	53.28(6)	N(1)–C(1)–Mo(2)	172.5(9)
Te(1)–Mo(2)–Mo(1)	58.03(3)	O(16)–C(16)–Fe(1)	140.1(9)
Fe(2)–Mo(2)–Mo(1)	58.68(3)	O(16)–C(16)–Fe(2)	140.7(9)
C(1)–Mo(2)–Fe(1)	130.0(3)	S(1)–Mo(2)–Fe(1)	93.86(6)

4. Supplementary material

Crystallographic data for the structural analysis have been deposited with the Cambridge Crystallographic Data Centre, CCDC nos. 181258 and 181259. Copies of this information may be obtained free of charge from The Director, CCDC, 12 Union Road, Cambridge CB2 1EZ, UK (Fax: +44-1223-336033; e-mail: deposit@ccdc. cam.ac.uk or http://www.ccdc.cam.ac.uk).

Acknowledgements

PM thanks the Council of Scientific and Industrial Research (India) for financial support, and the Royal Society of Chemistry for the award of a Journals Grant for International Authors. Financial support from the Natural Sciences and Engineering Research Council of Canada (NSERC) to MJM is gratefully acknowledged. JHK thanks NSERC and the Province of Ontario for graduate fellowships.

References

[1] P. Mathur, M.M. Hossain, A.L. Rheingold, Organometallics 13 (1994) 3909.
[2] P. Mathur, M.M. Hossain, S.B. Umbarkar, C.V.V. Satyanarayana, A.L. Rheingold, L.M. Liable-Sands, G.P.A. Yap, Organometallics 15 (1996) 1898.
[3] P. Mathur, S. Ghose, M.M. Hossain, C.V.V. Satyanarayana, M.F. Mahon, J. Organomet. Chem. 543 (1997) 189.
[4] L.E. Bogan Jr., T.B. Rauchfuss, A.L. Rheingold, J. Am. Chem. Soc. 107 (1985) 3843.
[5] P. Mathur, S. Ghose, M.M. Hossain, H. Vahrenkamp, J. Organomet. Chem. 538 (1997) 185.
[6] P. Mathur, S. Ghose, M.M. Hossain, P.B. Hitchcock, J.F. Nixon, J. Organomet. Chem. 542 (1997) 265.

[7] (a) P. Mathur, S. Ghose, M.M. Hossain, C.V.V. Satyanarayana, J.E. Drake, J. Organomet. Chem. 557 (1998) 219;
(b) P. Mathur, S. Ghose, R. Trivedi, M. Gelinsky, M. Rombach, H. Vahrenkamp, S. Banerjee, R. Philip, G.R. Kumar, J. Organomet. Chem. 595 (2000) 140.
[8] J.-M. Bassett, D.E. Berry, G.K. Barker, M. Green, J.A.K. Howard, F.G.A. Stone, J. Chem. Soc., Dalton Trans. (1979) 1003.
[9] R. Alvarez, E. Carmona, J.M. Marin, M.L. Poveda, E. Guetierrez-Puebla, A. Monge, J. Am. Chem. Soc. 108 (1986) 2286.
[10] SMART, Release 5.611, Bruker AXS Inc., Madison, WI 53711, 2000.
[11] SAINT, Release 6.02a, Bruker AXS Inc., Madison, WI 53711, 2000.
[12] G.M. Sheldrick, SADABS, Version 2.03, 2000.
[13] G.M. Sheldrick, SHELXTL, Version 5.1, Bruker AXS Inc., Madison, WI 53711, 1998.